A Numerical Study of Wavenumber Selection in Finite-Amplitude Rayleigh Convection

YOSHIMITSU OGURA

Laboratory for Atmospheric Research, University of Illinois, Urbana

(Manuscript received 2 October 1970, in revised form 1 March 1971)

ABSTRACT

Numerical integrations are performed for the equations governing two-dimensional convection flows in a fluid layer confined between two horizontal parallel plates and heated uniformly from below with free surface boundary conditions at the bottom and top of the fluid. In comparison with several previous works using a similar approach, a special feature in this work is that a large horizontal domain (10 times the critical wavelength or 28.28 times the height) is covered by the grid net so that the preferred mode of finite-amplitude convection flows is investigated.

The Rayleigh number covered here is less than four times the critical Rayleigh number. Either random or sinusoidal perturbations with various wavelengths and with various amplitudes are introduced to initiate the motion. In all cases considered, the system achieves an approximate steady state. It is found that: 1) steady-state solutions are not determined uniquely by only the Rayleigh and Prandtl numbers, but also by the initial conditions; 2) a second stability curve or a nonlinear stability curve exists as the dividing line between those cells which exhibit size-adjustment toward a more preferred mode and those which do not; 3) the preferred modes in steady-state solutions depend not only on the wavelength of the initial sinusoidal perturbations but also on their amplitudes; and 4) the extremum principle, such as the maximum heat transport, may be inapplicable in determining the preferred mode.

1. Introduction

When a layer of fluid is heated uniformly from below and cooled from above and the temperature difference between the top and bottom of the fluid layer (or more generally the Rayleigh number) exceeds a critical value, buoyancy-generated convection motions take place. The onset of such flows (known as the Rayleigh stability problem) has been thoroughly studied experimentally and theoretically. Fig. 1 shows the critical Rayleigh number as a function of horizontal wavenumber a at onset as derived by the linear stability analysis with free-free surface boundary conditions. Above the critical Rayleigh number, exponentially growing solutions are possible. The isopleths of the exponential growth rate σ in arbitrary units are also included in Fig. 1 for the first mode in the vertical (the notation N in Fig. 1 will be defined later).

Our understanding of finite-amplitude flows at supercritical conditions is, however, not complete. One of the problems which has been attracting interest recently is the manifold of steady solutions for each point in parameter space and the selection from this set. In other words, any modes above the critical stability curve ($\sigma=0$) in Fig. 1 are allowed to grow according to linear stability analysis, and under certain circumstances a steady-state solution to the equations of motion may not be determined uniquely by the steady-state boundary conditions. The questions we ask are what modes can be expected to exist in finite-amplitude, steady-state flows and whether these modes bear any relationship to the linear modes.

Saltzman (1962) was the first to apply a numerical method to investigate two-dimensional, finite-amplitude, steady-state Rayleigh convection as an initial-value problem. He expanded the variables in a double Fourier series and truncated the system by taking into account only a limited number of terms. The amplitudes of the eigenfunctions were evaluated by numerical integration of the resulting nonlinear equations. Using the ratio λ of the Rayleigh number to the critical Rayleigh number as a parameter, he con-

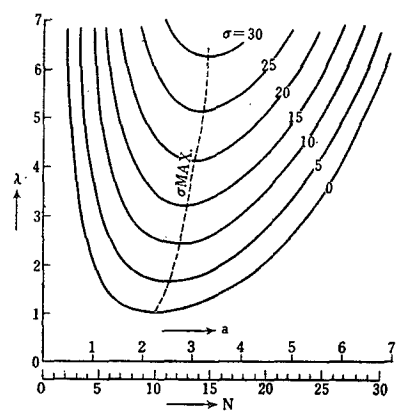

FIG. 1. Marginal stability curve (σ_{max}) and isopleths for various exponential growth rates (σ) in arbitrary units.

cluded for $1\leqslant\lambda\leqslant 2.125$ that the Rayleigh mode is present, whereas for $2.125<\lambda<10$ a smaller horizontal scale of cellular convection exists.

Using Saltzman's truncated system, however, Ogura and Yagihashi (1969b) demonstrated that a different mode can be present at finite-amplitude steady states for the same Rayleigh number, with the selection of the mode being determined by the relative magnitudes of the initial amplitudes of selected harmonics. They (Ogura and Yagihashi, 1969a) further confirmed this conclusion by integrating the full nonlinear equations for two-dimensional Rayleigh convection as an initial-value problem.

On the other hand, Chen and Whitehead (1968) showed experimentally that two-dimensional cells with width-depth ratios close to 2 are stable at the supercritical Rayleigh number investigated, whereas cells whose width-depth ratios are moderately too large or too small tend to undergo size adjustment toward a preferred value of about 2.2. A similar conclusion was also reached by Ogura and Tsu (1970).

Similar to Rayleigh convection in many aspects are the Taylor vortices which occur in the annular space between coaxial rotating cylinders. Coles (1965) showed experimentally that the wavenumber of steady-state Taylor vortices at supercritical conditions is not unique. Extending Coles' experiment, Snyder (1969) showed that the non-uniqueness observed by Coles in doubly periodic flows occurs also in the rotating symmetric case and that the wavenumber is determined uniquely by the initial conditions of the system. Snyder's paper also includes an excellent review of selection problems.

Since Saltzman's work, referred to above, several numerical experiments have been reported in which the full nonlinear equations are integrated as an initial-value problem (Deardorff, 1964; Herring, 1964; Fromm, 1965; Deardorff and Willis, 1965; Veronis, 1966; Chorin, 1966; Foster, 1969; Ogura and Yagihashi, 1969a). The work has been restricted for the most part to two spatial dimensions. For computations of this sort, one has to select a horizontal dimension for the computing grid and specify the boundary conditions at the edges. Two different boundary conditions have been applied; i.e., the ends of the interval are considered as physical boundaries or cyclic conditions are imposed. In either case, the domain of the integration has been confined to one or two wavelength strips in all previously reported works, except that of Deardorff and Willis (1965).[1] For the purpose of investigating the preferred mode of convection flows, this is not satisfactory.

The purpose of this paper is to report the result of a numerical investigation of the preferred modes of two-dimensional cellular convection flows. Linear stability analysis predicts that the width-height ratio of cells at the onset of convection is $2\times 2^{\frac{1}{2}}$ when free boundary conditions are applied at the top and bottom of the fluid layer. The horizontal domain in this work is chosen to be $20\times 2^{\frac{1}{2}}$ so that the fluid can accommodate 10 pairs of cells at the marginal state. The number of grid points in the horizontal direction was 128 to give a sufficient resolution to cells of this and neighboring wavenumbers.

[1] Since their primary interest was in the investigation of the effect of two-dimensionality on the suppression of thermal turbulence, their calculation was made at the Rayleigh number of 6.75×10^5, very high compared to the critical Rayleigh number of 1708.

2. Mathematical model

We consider two-dimensional motions in a layer of fluid bounded by parallel horizontal plates with separation d. The coordinate system (x,y,z) is used with the z axis vertical. All dependent variables are assumed to be independent of the x axis. The lower boundary $(z=0)$ of the fluid is maintained at temperature T_0 and the temperature of the upper boundary $(z=d)$ is $T_0-\Delta T$. With the Boussinesq approximation, the equations for the conservation of momentum, heat and mass are

$$\frac{\partial v}{\partial t}+v\frac{\partial v}{\partial y}+w\frac{\partial v}{\partial z}=-\frac{1}{\rho_0}\frac{\partial p}{\partial y}+\nu\nabla^2 v, \tag{2.1}$$

$$\frac{\partial w}{\partial t}+v\frac{\partial w}{\partial y}+w\frac{\partial w}{\partial z}=-\frac{1}{\rho_0}\frac{\partial p}{\partial z}+\nu\nabla^2 w+\alpha g T, \tag{2.2}$$

$$\frac{\partial T}{\partial t}+v\frac{\partial T}{\partial y}+w\frac{\partial T}{\partial z}=\kappa\nabla^2 T, \tag{2.3}$$

$$\frac{\partial v}{\partial y}+\frac{\partial w}{\partial z}=0, \tag{2.4}$$

where v,w are the velocity components along the y and z axes, respectively, T temperature, p pressure (deviation from hydrostatic equilibrium), ρ_0 constant density, ν the kinematic viscosity, κ the thermometric diffusivity, α the coefficient of volume expansion, g the acceleration of gravity and $\nabla^2=\partial^2/\partial y^2+\partial^2/\partial z^2$.

We eliminate the pressure term from (2.1) and (2.2) by cross-differentiation and then nondimensionalize the governing equations by using d, d^2/κ and ΔT as scale factors for length, time and temperature, respectively. The flows are then characterized by the nondimensional parameters:

$$[\text{Rayleigh number}]\quad \mathrm{Ra}=\frac{g\alpha\Delta T d^3}{\kappa\nu}$$

$$[\text{Prandtl number}]\quad \mathrm{Pr}=\frac{\nu}{\kappa}$$

The governing equations are then written in nondimensional form as

$$\frac{\partial \xi}{\partial t}+v\frac{\partial \xi}{\partial y}+w\frac{\partial \xi}{\partial z}=\mathrm{Pr}\nabla^2\xi+\mathrm{Ra}\,\mathrm{Pr}\frac{\partial \theta}{\partial y}, \tag{2.5}$$

$$\frac{\partial\theta}{\partial t}+v\frac{\partial\theta}{\partial y}+w\left(\frac{\partial\theta}{\partial z}-\mathrm{Ra}\right)=\nabla^2\theta. \tag{2.6}$$

Hereafter all quantities should be understood to be expressed in nondimensional form, unless otherwise stated. In the above equations, the x component of vorticity, ξ, is given by

$$\xi=\frac{\partial w}{\partial y}-\frac{\partial v}{\partial z}=\nabla^2\psi, \tag{2.7}$$

and θ is the deviation of temperature from the basic temperature distribution, which has a uniform vertical temperature gradient $\Delta T/d$. The nondimensional streamfunction ψ is defined by

$$v=-\frac{\partial\psi}{\partial z},\quad w=\frac{\partial\psi}{\partial y}.$$

For the sake of mathematical simplicity, we apply free boundary conditions at the bottom and top boundaries. Thus, the conditions are

$$\psi=\nabla^2\psi=\theta=0 \quad \text{at } z=0,1. \tag{2.8}$$

The lateral boundary conditions we apply are that the motion is cyclic over the horizontal space interval L.

The finite-difference schemes we used to integrate Eqs. (2.5) and (2.6) are essentially the same as those used by Lilly (1964) and Ogura and Yagihashi (1969a), except that the diffusion terms are evaluated by using the DuFort-Frankel scheme. This permits use of a larger time increment than that required if the diffusion terms are evaluated by the forward time differences without violating linear computational stability. The schemes used here preserve the total energy of the system and the variance of temperature in the finite-difference form in a manner analogous to that of the continuous system.

The method we used to solve the Poisson equation (2.7), with cyclic lateral boundary conditions and the top and bottom boundary conditions given by (2.8), is as follows. First, we expand ξ and ψ into trigonometric series in the y direction and substitute them into Eq. (2.7). Eq. (2.7) is then transformed into a set of simultaneous ordinary second-order differential equations for the amplitudes of Fourier expansions as functions of z. This set of equations is then solved with the boundary conditions (2.8) by the method described by Todd (1962, p. 394) or Richtmyer and Morton (1967, p. 198). The values of ψ at each grid point are finally calculated by synthesizing the trigonometric series.

In trigonometric decomposition and synthesis, the fast Fourier transform algorithm proposed by Cooley and Tukey (1965) is applicable. This algorithm reduces the amount of multiplication in the trigonometric transforms by taking advantage of the symmetry properties of the trigonometric functions. In our calculations a refined technique developed by Takahashi (1968) was used which is applicable when the Fourier amplitudes are real. Some details of the method outlined above are given in a paper by Ogura (1969).

TABLE 1. Initial perturbations, time span covered by numerical integrations, number of cells, and Nusselt numbers in the resulting steady states.

Case	λ	Initial perturbations	Time span	N	Nusselt no.
1	2	random	15.6	11	2.04
2	2	sinusoidal ($N=5$, $A=0.01$)	24.0	11	2.04
3	2	sinusoidal ($N=6$, $A=0.01$)	9.6	6	1.64
4	2	sinusoidal ($N=8$, $A=0.01$)	6.8	8	1.97
5	2	sinusoidal ($N=10$, $A=0.01$)	63.8	10	2.06
6	2	sinusoidal ($N=11$, $A=0.01$)	8.0	11	2.04
7	2	sinusoidal ($N=16$, $A=0.01$)	5.6	16	1.46
8	2	sinusoidal ($N=17$, $A=0.01$)	9.1	11	2.04
9	2	sinusoidal ($N=18$, $A=0.01$)	8.0	11	2.04
10	2	sinusoidal ($N=19$, $A=0.01$)	8.0	11	2.04
11	2	sinusoidal ($N=5$, $A=0.1$)	12.0	10	2.06
12	2	sinusoidal ($N=5$, $A=0.2$)	14.5	9	2.05
13	2	sinusoidal ($N=5$, $A=0.4$)	20.0	9	2.05
14	4	random	21.0	12	2.94
15	4	sinusoidal ($N=3$, $A=0.01$)	10.0	12	2.94
16	4	sinusoidal ($N=4$, $A=0.01$)	4.0	12	2.94
17	4	sinusoidal ($N=5$, $A=0.01$)	4.0	5	2.31
18	4	sinusoidal ($N=9$, $A=0.05$)	4.0	9	2.95
19	4	sinusoidal ($N=10$, $A=0.05$)	4.0	10	2.97
20	4	sinusoidal ($N=11$, $A=0.05$)	4.0	11	2.97
21	4	sinusoidal ($N=14$, $A=0.05$)	2.0	14	2.82
22	4	sinusoidal ($N=16$, $A=0.05$)	2.0	16	2.61

As was mentioned in the Introduction, the purpose of this work is to investigate the preferred mode of cellular convection at supercritical conditions. For this purpose, it is essential to have a large horizontal dimension for our working fluid so that many modes can be accommodated in the fluid. In this series of numerical integrations, we assigned a value of 28.29 to L (the nondimensional horizontal span over which the cyclic lateral boundary conditions were imposed). This value is 10 times the critical wavelength at the marginal Rayleigh number so that our working fluid is able to accommodate 10 pairs of convection cells at the onset of convection. This choice of L was made on the basis of Snyder's conclusion that horizontal dimensions of less than five wavelengths are not suitable if end effects are to be avoided.

It was found convenient to express the horizontal wavenumber (a) of convection cells in terms of the number of pairs of cells (N); the relation between them is

$$a=\frac{2\pi N}{L}=\frac{2\pi N}{28.29}.$$

Fig. 1 shows the unstable region in a,λ or N,λ space. Included in this figure are isopleths of exponential growth rate as calculated by linear stability analysis.

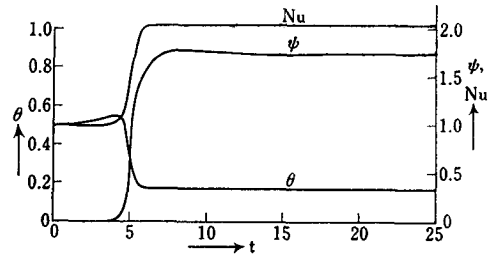

FIG. 2. Changes with time of the streamfunction (ψ) and temperature (θ) at a selected point, and the change of the Nusselt number (Nu) at the middle level for case 2.

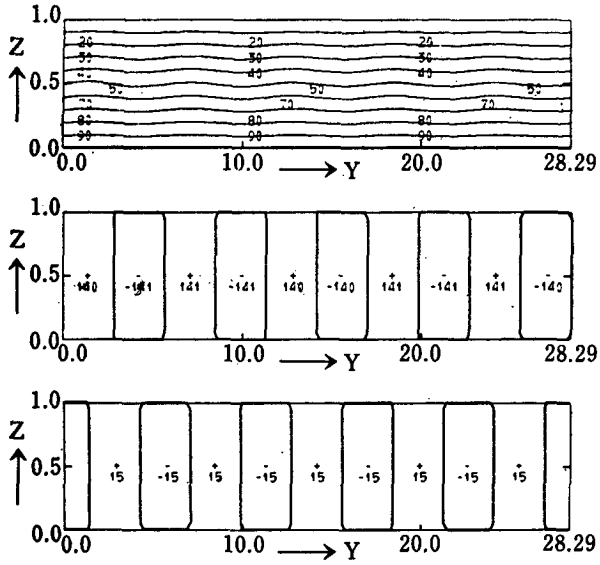

FIG. 3. Isotherms (upper), isopleths of temperature deviation from the horizontally averaged temperature (middle), and isopleths of streamfunction (lower), at $t=1.75$ for case 2.

We observe, when $\lambda=2$ for example, that the number of pairs of cells in the range $N=5$ ($a=1.11$) to $N=19$ ($a=4.22$) is in the unstable region; therefore, these cells are allowed to grow according to the linear stability analysis.

The number of grid points in the horizontal was 2^7 ($=128$). This choice was made to give a sufficient horizontal resolution for convection cells considered here and at the same time to take advantage of the fast Fourier transforms. The number of grid points in the vertical was 20. It was shown in our previous study (Ogura and Yagihashi, 1969a) that this number gives a sufficient vertical resolution for convection in the range of Rayleigh number we consider here ($\lambda \leqslant 4$). Different time increments Δt were used to permit the integration to proceed without any computational instability. The range of Δt applied was between 0.004 and 0.01. In some cases, the computations were repeated with Δt as small as 0.00025 to make sure that the resulting flow patterns were not affected by the choice of Δt.

Table 1 gives relevant information concerning the cases investigated. In the numerical approach we used, the calculation begins with no convective motion but with an initial uniform supercritical vertical temperature gradient. Motion is initiated by introducing into the temperature field either a random perturbation of the order of (1/100) in magnitude or a sinusoidal perturbation given by

$$\theta = A \sin\frac{2\pi N y}{L} \sin\pi z,$$

with the amplitude denoted by A.

In the integration of the equations, the motion invariably appeared to settle down to a steady state. By definition, the nondimensional vertical heat flux (Nusselt number) must be independent of the vertical

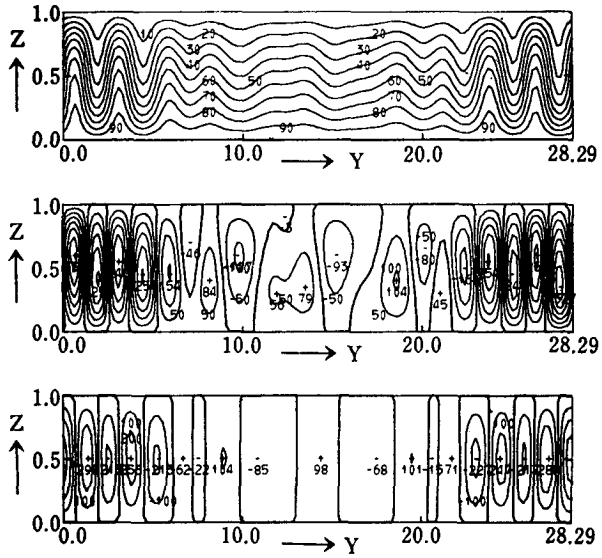

FIG. 4. Same as Fig. 3 except for $t=4.125$.

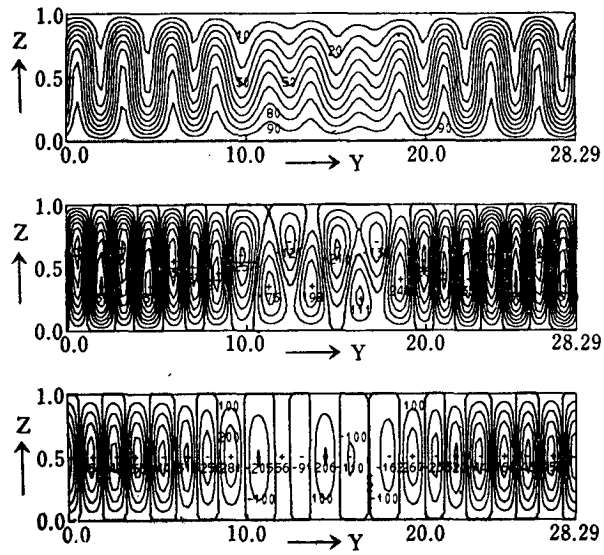

FIG. 5. Same as Fig. 3 except for $t=4.5$.

coordinate z in the steady state. Our previous experience (Ogura and Yagihashi, 1969a) indicates that the Nusselt number is the variable which approaches the steady state last. For this reason, all time integrations were continued until the vertical distribution of the heat flux became independent of z in the main portion of the fluid layer within an error of less than 1.5% in the cases for $\lambda=2$. This accuracy was reduced to 3% in cases for $\lambda=4$ simply to save computer time. However, in some cases the calculations were continued much further than required by this criterion to make sure that there would be no possibility of transition from the present mode to another. Included in Table 1 is the time when the computations were discontinued for each case.

In all cases the Prandtl number was given a value of 0.713, corresponding to air.

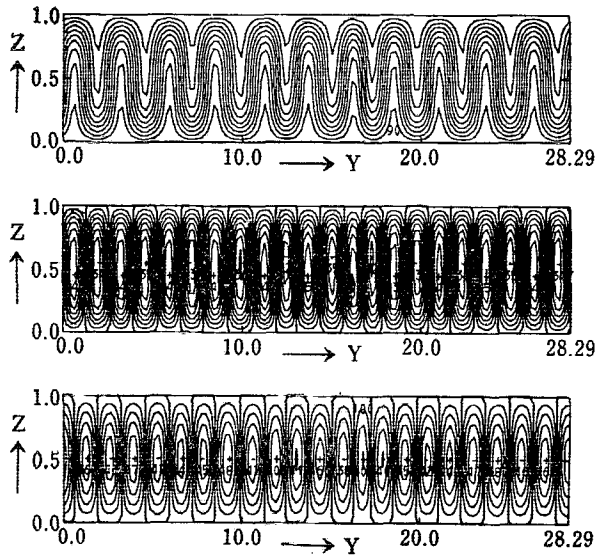

FIG. 6. Same as Fig. 3 except for $t=5.0$.

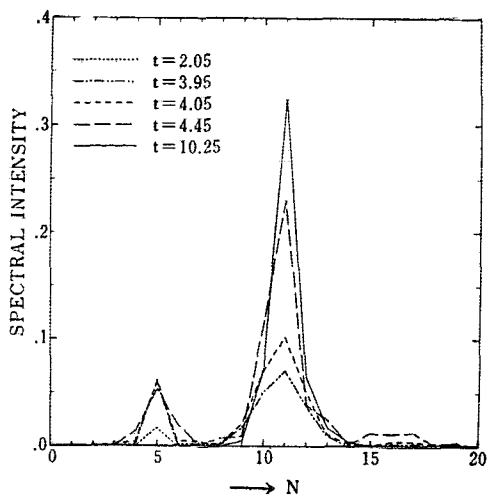

FIG. 7. The spectral density distributions at various times for case 2.

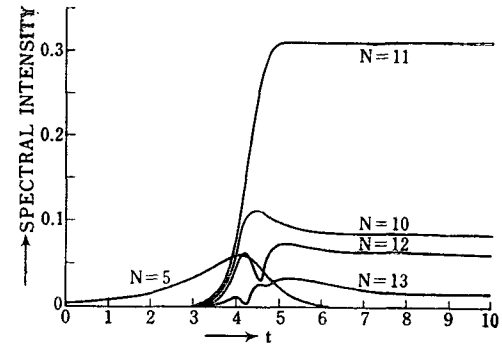

FIG. 8. Changes of the spectral intensities of various wavenumbers (N) with time for case 2.

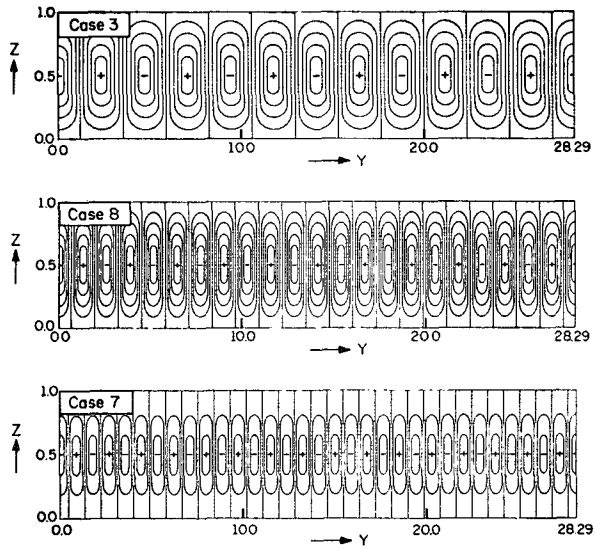

FIG. 9. Steady-state flow pattern for three cases with $\lambda=2$.

3. Results and discussions

An example of the evolution of convection flows with time is shown in Figs. 2–8 for case 2. Fig. 2 shows the changes with time of ψ and θ at a selected point ($y=14.15$, $z=0.5$) and the Nusselt number (Nu) calculated at $z=0.5$. We observe that these values attain approximately steady states somewhere near $t=10$.

The temperature field and the streamfunction field at various times are shown in Figs. 3–6. We observe that the initial fields of 5 pairs of cells keep their original patterns (but with slightly increasing amplitudes) until approximately $t=3.5$. A rather rapid change of patterns then takes place and by about $t=5$ a flow with 11 pairs of cells is established. After that no appreciable change in the flow pattern is observed.

This change of flow pattern is most clearly illustrated with the time-changing spectral density distributions of temperature (Fig. 7). Fig. 8 shows the changes with time of the spectral intensities for those wavenumbers which are present at the steady state. In Figs. 7 and 8 the ordinate is the square root of the sum of squared

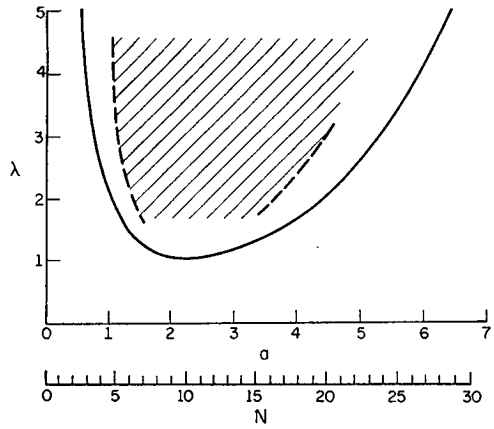

FIG. 10. Summary of size-adjustment observations as functions of horizontal wavenumber and Rayleigh number. The solid line indicates the neutral curve for convection onset obtained from the linear stability problem; modes in the shaded region do not exhibit size-adjustment.

amplitudes of the horizontal Fourier harmonics for the temperature field calculated at $z=0.5$. Our initial conditions in this case are such that the line spectrum is present at $N=5$ with an intensity of 0.01. This intensity increases with time until approximately $t=4$ and then vanishes. Meanwhile, the intensities at $N=11$ and neighboring wavenumbers are increasing. This rapid increase is particularly pronounced at $N=11$ between $t=4$ and 5.

Fig. 9 shows some examples of steady-state flow patterns. Because all of these patterns are produced under the same steady boundary conditions, this figure may serve to demonstrate a manifold of steady-state solutions of the Boussinesq convection equations.

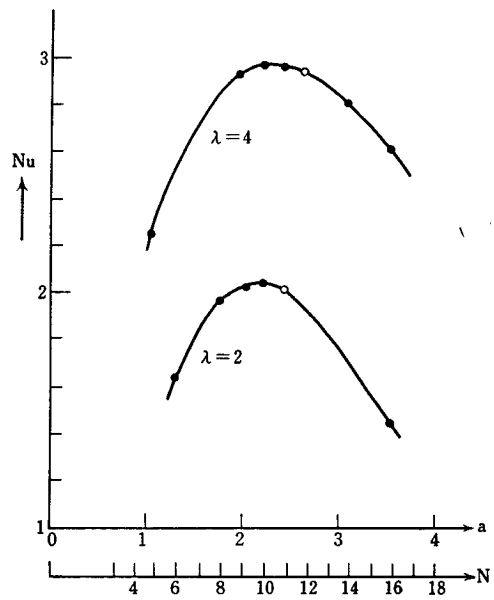

FIG. 11. Nusselt numbers as functions of wavenumber for $\lambda=2$ and $\lambda=4$.

We shall now go to the question we asked in Section 1: What modes of cellular convection are present in finite-amplitude, steady-state flows? Table 1 also includes the number of pairs of cells resulting from the numerical integration in the steady state. The results for cases 1–10 indicate the following in cases for $\lambda=2$: 1) when a random perturbation is introduced to initiate motion, 11 pairs of cells are present in the steady state (case 1); 2) for each case where a sinusoidal perturbation with $N=5$, 17, 18 and 19 and with $A=0.01$ is introduced (cases 2, 8, 9 and 10), the initial flow undergoes the size-adjustment as described above and finally settles down to a steady-state flow which is the same as case 1, i.e., 11 pairs of cells; and 3) for a sinusoidal perturbation with N lying between 6 and 16 (cases 3, 4, 5, 6, 7 and 8), the initial mode remains unchanged.

The above results suggest that a secondary stability curve exists as the dividing line between those cells which exhibit size-adjustment and those which do not (Fig. 10). In other words, there is a band of allowed wavenumbers which is narrower than the band that can grow according to linear theory.

Similar tendencies may also be observed in cases where $\lambda=4$. The preferred mode when the motion is initiated by random perturbations (case 14) is 12 pairs. The second stability curve lies between $N=4$ and 5 because sinusoidal perturbations with $N=3$ (case 15) and $N=4$ (case 16) undergo size-adjustments but a perturbation with $N=5$ (case 17) does not. No attempt was made to determine the position of the secondary stability curve in the higher wavenumber side at $\lambda=4$ because it was suspected that our grid net might not give a sufficient resolution to cells of such high wavenumber.

The band inside the secondary stability curve is equally stable in the sense that the selection of a preferred wavenumber in this band is determined by the initial conditions. Malkus and Veronis (1958) suggested criteria for selection based on an extremum principle, one of the criteria being the principle of maximum heat transport. This principle selects one wavenumber regardless of the initial conditions and does not agree with the present results.

Fig. 11 shows the Nusselt number as a function of wavenumber. It is noted for $\lambda=2$ that the Nusselt

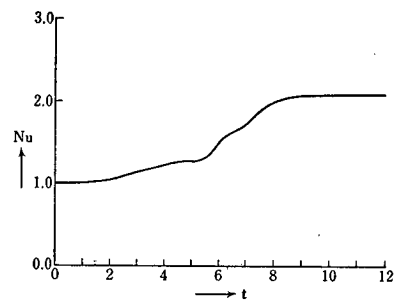

FIG. 12. Change of Nusselt number with time for case 11.

number takes its maximum value at $N=10$, whereas $N=11$ is the wavenumber selected when a random perturbation or sinusoidal perturbations with small amplitudes and with wavenumbers outside the stable band are introduced. Similarly, for $\lambda=4$, the Nusselt number takes a maximum at N between 10 and 11 whereas $N=12$ is the preferred mode. The present results indicate that there is a preferred mode for each λ in the sense that modes lying between the primary and secondary stability curves tend to settle down to this mode. This mode, however, does not give the maximum heat transport.

However, there are more complexities in the steady-state solutions. Let us consider cases 11, 12 and 13 where the motions are initiated by introducing sinusoidal perturbations of larger amplitudes than in the other cases. Figs. 12 and 13 show the changes with time of the heat flux and the amplitude of each harmonic, respectively, for case 11. We observe in Fig. 13 that the amplitude of the initial mode 5 first decreases, then increases, reaches a maximum with quite a large value, then finally decays. Meanwhile, modes 6, 9, 10 and 11 are excited, but all these modes appear to decay except for mode 10. Although Fig. 12 shows that the Nusselt number attained a steady-state value, Fig. 13 indicates that the computation was not continued long enough so that the spectrum in the steady state could be confirmed. Nevertheless, the result appears to indicate that mode 10 is the dominant one, in contrast to case 2 where mode 11 is the dominant one. The only difference between this case and case 2 is in the amplitudes of the initial sinusoidal perturbations ($A=0.01$ for case 2 and $A=0.1$ for case 11).

Fig. 14 shows the result for case 12 where the amplitude of the initial perturbation is increased to 0.2 in contrast to 0.1 in case 11. Apparently mode 9 is the preferred mode in the case.

Fig. 15 shows the result for case 13 where the amplitude is 0.4. Again mode 9 is the preferred one in the steady state. The variations of the intensity of other modes with time are not shown in this figure except for mode 10, because they are considerably smaller than

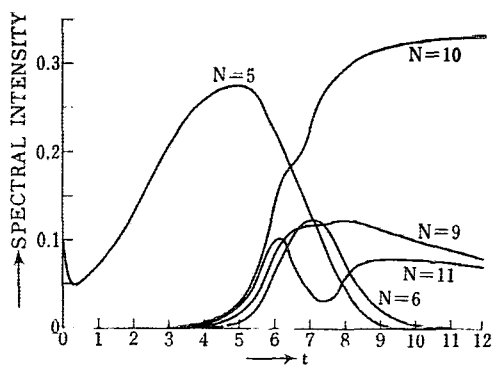

FIG. 13. Changes of spectral intensities with time for case 11.

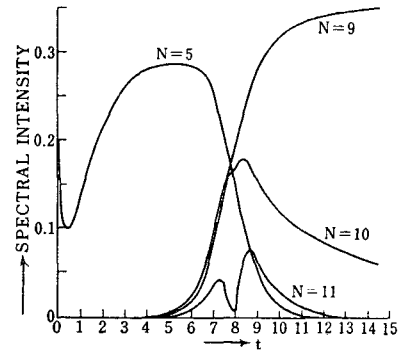

FIG. 14. Change of spectral intensities with time for case 12.

that for mode 10; the maximum intensity for mode 11 is 0.05 and that for mode 8 is 0.045, for example.

In connection with Figs. 13 and 14, we may refer to our previous result (Ogura and Yagihashi, 1969b) which indicates that slightly different initial conditions give rise to motions of different modes[2] at the same Rayleigh number for a highly truncated system. For example, in a case where the initial amplitude of cells of mode 3 is 5×10^{-4} and that of mode 4 is 1.60×10^{-4}, only mode 3 is present at the steady state at $\lambda=5$, whereas mode 4 establishes itself as the only mode present at the steady state in a case where the initial amplitude of mode 3 is held unchanged and that of mode 4 is slightly increased to 1.65×10^{-4}.

It may therefore be inferred from the result obtained in cases 11 and 12 that there is a dividing value between 0.1 and 0.2 for the initial amplitude (A_5) of $N=5$ so that if A_5 is smaller than this value, mode 10 is preferred, whereas mode 9 is preferred if A_5 is larger than this value.

4. Concluding remarks

In this paper it was found that: 1) finite-amplitude steady-state solutions for Rayleigh convection are not

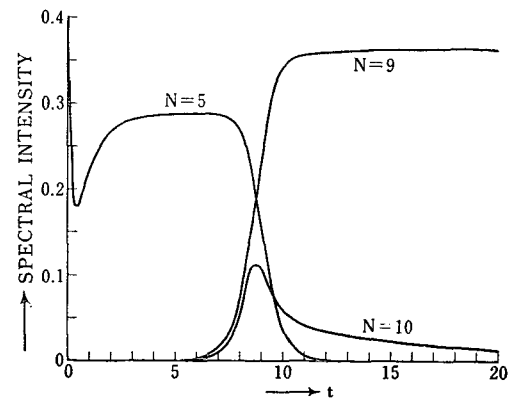

FIG. 15. Change of spectral intensities with time for case 13.

[2] Here mode 3 corresponds to the linear mode (nondimensional wavelength = 2.828) and the nondimensional wavelength for mode 4 is 2.121.

determined uniquely by only the Rayleigh number and Prandtl numbers but are also determined by the initial conditions; 2) a second stability curve or a nonlinear stability curve exists as the dividing line between those cells which undergo size-adjustment from an initial mode toward a more preferred mode and those which do not; 3) the preferred modes in steady-state solutions depend, however, not only on the wavelength of the initial perturbations but also on their amplitudes; and 4) an extremum principle such as the maximum heat transport predicts a single mode present in a steady state for a given Rayleigh number whereas the present result indicates that there is a band of allowed wavenumbers.

In connection with the last item, a question may be asked whether or not the steady-state solutions resulting from the numerical calculations are stable for perturbations of small amplitudes. No numerical experiment has been done in this work to answer this question. The implication, however, is that they are stable so long as the perturbations are two-dimensional because the steady-state solutions are obtained as a result of nonlinear interactions between different modes. The result in our previous paper (Ogura and Yagihashi, 1969b) also appears to support this conjecture, although an extremely truncated system was applied in the previous work.

As to the two-dimensionality of the motions discussed here, we introduced this simplification mainly because of the limitation of available computer capability. This was also done because recent investigations have shown that, when a layer of fluid is heated uniformly from below and cooled from above, the resulting convection takes place as a pattern of two-dimensional rolls. Koschmieder (1966) showed experimentally, when the lateral boundaries were circular, that the pattern consisted of concentric rolls (cylindrical symmetry) and when the boundaries formed a square, the pattern tended to establish two-dimensional rolls. Schlüter *et al.* (1965) treated the theoretical problem by taking as a basic state a fluid with a steady pattern of cellular motions and then perturbing the given pattern with an arbitrary disturbance. They showed that the only pattern which is stable to the perturbations is a system of convection rolls.[3]

More recently, Krishnamurti (1970) found, for a fluid layer occupying a region 51 cm by 49 cm, that the flow pattern consisted of two-dimensional rolls for Rayleigh numbers $\lesssim 12$ times the critical Rayleigh number. For Rayleigh numbers exceeding this value, a change in the flow pattern from two-dimensional rolls to three-dimensional flow is observed with no definite Prandtl number dependence in the range $10 < \mathrm{Pr} < 10^4$.

[3] Schlüter *et al.* (1965) considered a fluid layer of infinite horizontal extent. More recently, Davis (1967) and Segel (1969) discussed the effect of vertical boundaries on convection in a thin fluid layer confined in a box. It is found that finite rolls (cells with two non-zero velocity components dependent on all three spatial variables) with axes parallel to the shorter side are predicted.

Next, some remarks will be made on the dependence of the preferred size of convection cells upon the supercritical Rayleigh number. Koschmieder (1966, 1969) showed experimentally that the wavelength of convective motions on a uniformly heated plane increases with increasing supercritical Rayleigh numbers. For example, he observed 13 concentric circular rolls present in a circular chamber at a Rayleigh number of 1.06 R_c, whereas 11 concentric rolls were observed at approximately 3 R_c in a silicone oil layer. A similar tendency was also observed by Deardorff and Willis (1965) for two-dimensional convection in an air layer confined between two horizontal plates and vertical barriers. Their Rayleigh numbers were very high, in the range between 1.6×10^6 and 1.5×10^7. The recent investigation by Krishnamurti (1970) also confirms this tendency.

On the other hand, Ukaji and Sawada (1969) showed experimentally that the wavelength decreases with increasing supercritical Rayleigh numbers for convective motions in a silicone oil layer confined in a chamber which was 284 mm long, 42 mm high and 9.8 mm thick. Their Rayleigh numbers were in the range from 4.9×10^4 up to 1.0×10^7. They estimated that the critical Rayleigh number[4] for a fluid layer confined in their chamber was 2.8×10^4.

Finally, Mori and Uchida (1966) showed that the size of two-dimensional cells observed in a flow between two horizontal plates is approximately the same as that predicted by a linear stability theory for the range of the Rayleigh number $4120 < \mathrm{Ra} < 10{,}680$, as long as the separation between two plates is less than 15 mm.

On the theoretical side, Schlüter *et al.* (1965) have computed the effects of finite-amplitude convection with regard to the preferred mode in the case of a fluid layer of infinite horizontal extent. They find that the wavenumber preferred in finite-amplitude convection increases with increasing supercritical Rayleigh number. On the other hand, Newell *et al.* (1970) discussed the initial convective phase of a fluid as a statistical initial-value problem. They concluded that a natural statistical selection process chooses from the initial disorder a perfectly ordered field of single rolls and the scale of this roll is the scale corresponding to the most critical wavenumber obtained from the linear stability problem.

Davis (1968) then discussed the dependence of preferred wavenumber upon the Rayleigh number at finite amplitude for convection in a box. He applied Stuart's shape assumption and assumed that the preferred mode is that which convects the most heat. It is found that the preferred number of finite roll cells tends to decrease with increasing Rayleigh number in contradiction to the behavior in an infinite layer.

The present work assumed two-dimensionality for the motion and applied cyclic lateral boundary condi-

[4] This increase of the critical Rayleigh number from that for a horizontally infinite fluid layer was attributed not only to the smallness of the width of their fluid layer but also to the finite thermal conductivity of the side walls (Ukaji and Matsuno, 1970).

tions. The convective motion discussed is therefore more like convection in a fluid of an infinite horizontal extent rather than that in a box. Wavenumbers of cells which resulted from random initial perturbations and those which give maximum heat transport are both found to increase with increasing Rayleigh number. It would be of interest, therefore, to extend this work to a three-dimensional case with rigid lateral boundary conditions. The three-dimensionality of the motion may be important because, even though two-dimensional motions are the final steady-state solutions, the path for getting to such solutions may require a three-dimensional flow and the metastable states discussed in the present paper may be modified if three-dimensional motions are allowed.

Acknowledgments. The author wishes to thank Miss Akiko Yagihashi for programming the computation, Mrs. Masako Ogura of the Center for Advanced Computation for providing us with a programming for the solution of Poisson's equation, Dr. Marvin A. Geller for reading the manuscript, and Mrs. Betty Wolfe for typing the manuscript.

This work was sponsored by the Atmospheric Sciences Section, National Science Foundation, under Grant GA-020328. The computations were done on the Control Data 6600 at the National Center for Atmospheric Research which is sponsored by the National Science Foundation.

REFERENCES

Chen, M. M., and J. A. Whitehead, 1968: Evolution of two-dimensional periodic Rayleigh convection cells of arbitrary wave-numbers. *J. Fluid Mech.*, **31**, 1–15.

Chorin, A. J., 1966: Numerical study of thermal convection in a fluid layer heated from below. AEC Research and Development Rept., TID-4500, Courant Institute of Mathematical Sciences, New York University, 85 pp.

Coles D., 1965: Transition in circular Couette flow. *J. Fluid Mech.*, **21**, 385–425.

Cooley, J. W., and J. W. Tukey, 1965: An algorithm for the machine calculation of complex Fourier series. *Math. Comput.*, **19**, 297–301.

Davis, S., 1967: Convection in a box: Linear theory. *J. Fluid Mech.*, **30**, 465–478.

——, 1968: Convection in a box: On the dependence of preferred wave-number upon the Rayleigh number at finite amplitude. *J. Fluid Mech.*, **32**, 619–624.

Deardorff, J. W., 1964: A numerical study of two-dimensional parallel-plate convection. *J. Atmos. Sci.*, **21**, 419–438.

——, and G. E. Willis, 1965: The effect of two-dimensionality on the suppression of thermal turbulence. *J. Fluid Mech.*, **23**, 337–353.

Foster, T. D., 1969: The effects of initial conditions and lateral boundaries on convection. *J. Fluid Mech.*, **37**, 81–94.

Fromm, J. E., 1965: Numerical solutions of the nonlinear equations for a heated fluid layer. *Phys. Fluids*, **8**, 1757–1769.

Herring, J. R., 1964: Investigation of problems in thermal convection: Rigid boundaries. *J. Atmos. Sci.*, **21**, 277–290.

Koschmieder, E. L., 1966: On convection on a uniformly heated plate. *Beitr. Phys. Atmos.*, **39**, 1–11.

——, 1967: On convection under an air surface. *J. Fluid Mech.*, **30**, 9–15.

——, 1969: On the wavelength of convective motions. *J. Fluid Mech.*, **35**, 527–530.

Krishnamurti, R., 1970: On the transition to turbulent convection. Part 1. The transition from two- to three-dimensional flow. *J. Fluid Mech.*, **42**, 295–307.

Lilly, D. K., 1964: Numerical solutions for the shape-preserving two-dimensional thermal convection element. *J. Atmos. Sci.*, **21**, 83–98.

Malkus, W. V. R., and G. Veronis, 1958: Finite-amplitude cellular convection. *J. Fluid Mech.*, **4**, 225–260.

Mori, Y., and Y. Uchida, 1966: Forced convective heat transfer between horizontal flat plates. *Intern. J. Heat Mass Transfer*, **9**, 803–817.

Newell, A. C., L. G. Lange and P. J. Aucoin, 1970: Random convection. *J. Fluid Mech.*, **40**, 513–542.

Ogura, M., 1969: A direct solution of Poisson's equation by dimension reduction method. *J. Meteor. Soc. Japan*, **47**, 319–323.

Ogura, Y., and A. Yagihashi, 1969a: A numerical study of convection rolls in a flow between horizontal parallel plates. *J. Meteor. Soc. Japan*, **47**, 205–218.

——, and ——, 1969b: On the degeneracy of finite-amplitude steady-state solutions for Bénard convection in a highly truncated system. *J. Meteor. Soc. Japan*, **47**, 437–445.

——, and H. Tsu, 1970: An experimental study of the wave-number selection for the finite-amplitude Rayleigh convection. *J. Meteor. Soc. Japan*, **48**, 400–404.

Richtmyer, R. D., and K. W. Morton, 1967: *Difference Methods for Initial-Value Problems*, 2nd. ed. New York, Interscience, 405 pp.

Saltzman, B., 1962: Finite-amplitude free convection as an initial value problem: I. *J. Atmos. Sci.*, **19**, 329–341.

Schlüter, A., D. Lortz and F. Busse, 1965: On the stability of steady finite amplitude convection. *J. Fluid Mech.*, **23**, 129–144.

Segel, L. A., 1969: Distant side-walls cause slow amplitude modulation of cellular convection. *J. Fluid Mech.*, **38**, 203–224.

Snyder, H. A., 1969: Wave-number selection at finite amplitude in rotating Couette flow. *J. Fluid Mech.*, **35**, 273–298.

Takahashi, H., 1968: Fast Fourier Transform. D6/TC/FFTR Library Subroutine, Computer Center, University of Tokyo.

Todd, J., 1962: *Survey of Numerical Analysis*. New York, McGraw-Hill, 582 pp.

Ukaji, K., and R. Sawada, 1969: The convective heat transport and the number of convection cells. *J. Meteor. Soc. Japan*, **47**, 451–456.

——, and T. Matsuno, 1970: Effect of lateral walls on the onset of convective motions. *J. Meteor. Soc. Japan*, **48**, 217–223.

Veronis, G., 1966: Large-amplitude Bénard convection. *J. Fluid Mech.*, **26**, 49–68.